

NO. 133 CRATER STATISTICS NEAR THE FLAMSTEED P RING

by R. FRYER AND C. TITULAER¹⁾

December 1, 1968

ABSTRACT

Previous work on the population curves and crater distribution in the vicinity of *Surveyor I* is reviewed and extended. A total-population curve is derived for craters ranging in size from centimeters to kilometers. Comparison is made with *Ranger* data covering an equivalent diameter range. The floor of the low ring Flamsteed P is found to be unusually young, younger than the surrounding mare; this is consistent with the recent hypotheses of O'Keefe and Fielder which regard the ring as a recent extrusive structure.

1. Introduction

Surveyor I landed at 06:17:37 GMT on June 2, 1966, at a point in Oceanus Procellarum with selenographic coordinates 2°45 S, 43°22 W (Whitaker 1968). The landing site lies in the northeast * quarter of the flat floor of a low ring structure known as Flamsteed P (Figs. 1-4) named after the sharp 20.6 km crater which lies upon the southern wall of the low ring, approximately 65 km south-southwest of the spacecraft. The area has been extensively mapped (Marshall 1963; ACIC Map No. AIC 75A, 1966).

"Ghost" rings of the type represented by Flamsteed P have often been assumed to ancient, eroded, and partially buried remnants of the walls of craters

existing prior to the formation of the maria in which they stand, without major subsequent modification having occurred. This hypothesis has recently been challenged (O'Keefe *et al* 1967; Fielder 1967) on the basis of *Orbiter* photographs. Both authors assume extrusion of lava from near-circular ring fractures in the mare surface (with no prior meteoritic impact having occurred to define the ring), O'Keefe *et al.* favoring a single eruption of very viscous lava; and Fielder finding evidence for successive flows. The case presented by Fielder has since been elaborated in a further paper (Guest and Fielder 1968) which includes a table of "elementary rings" having similar properties to Flamsteed P, and also suggests a number of terrestrial analogues. Many of the arguments presented in the two original papers are disputed by Hartmann (1967) and others, who conclude that the "flow" structure observed on the hills forming Flamsteed P may be the result of *slumping*, since it

¹ Present address: Observatoire de Paris, Section d'Astrophysique, 92 Meudon (Haute de Seine), France.

*The astronomical convention for map directions is used throughout this paper.

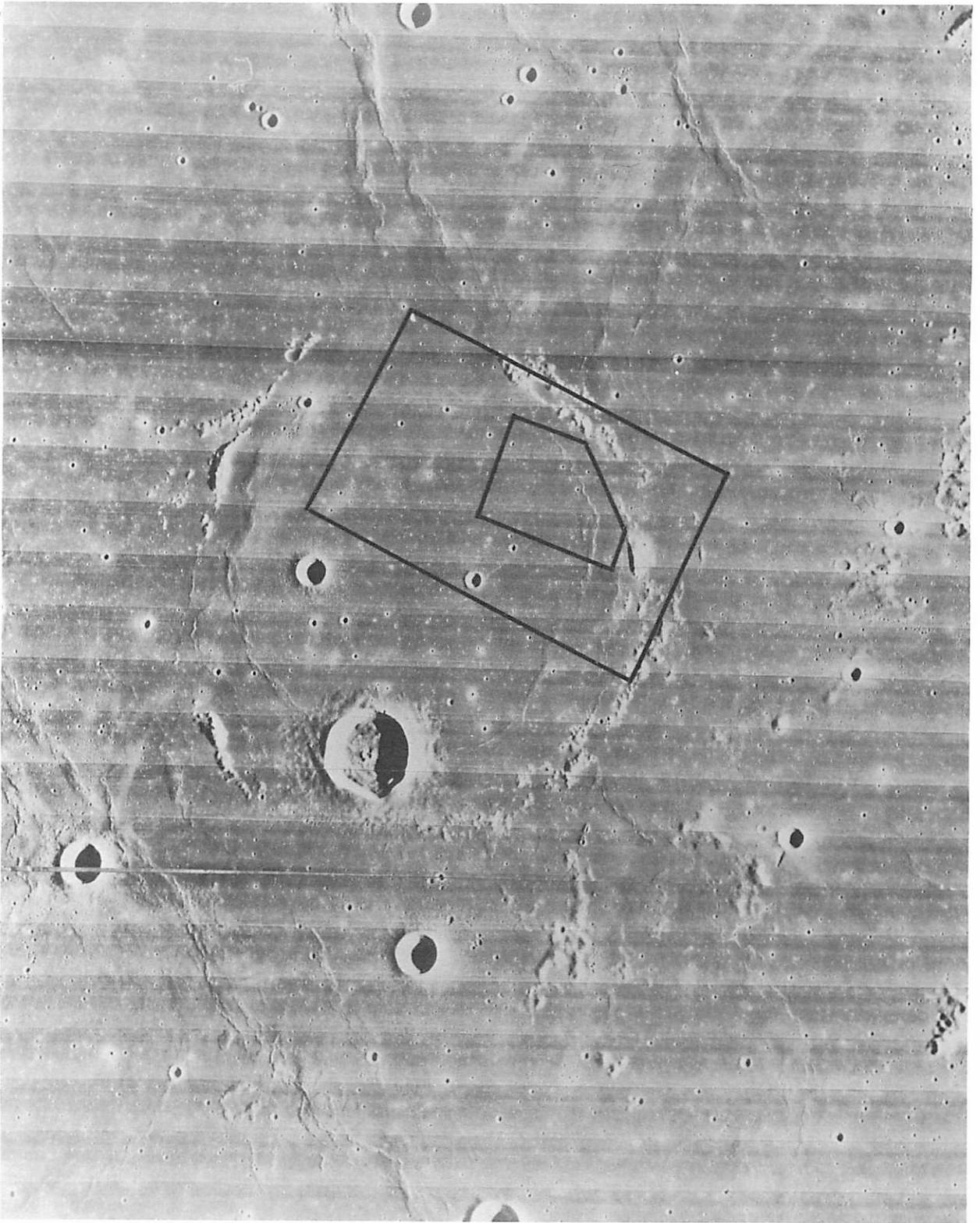


Fig. 1 Orbiter photograph IV-H-143. The larger marked area is area GA of Fielder *et al.* (1968). The smaller area was used in extending the crater population curve, and is shown in greater detail in Fig. 2. (NASA photograph).

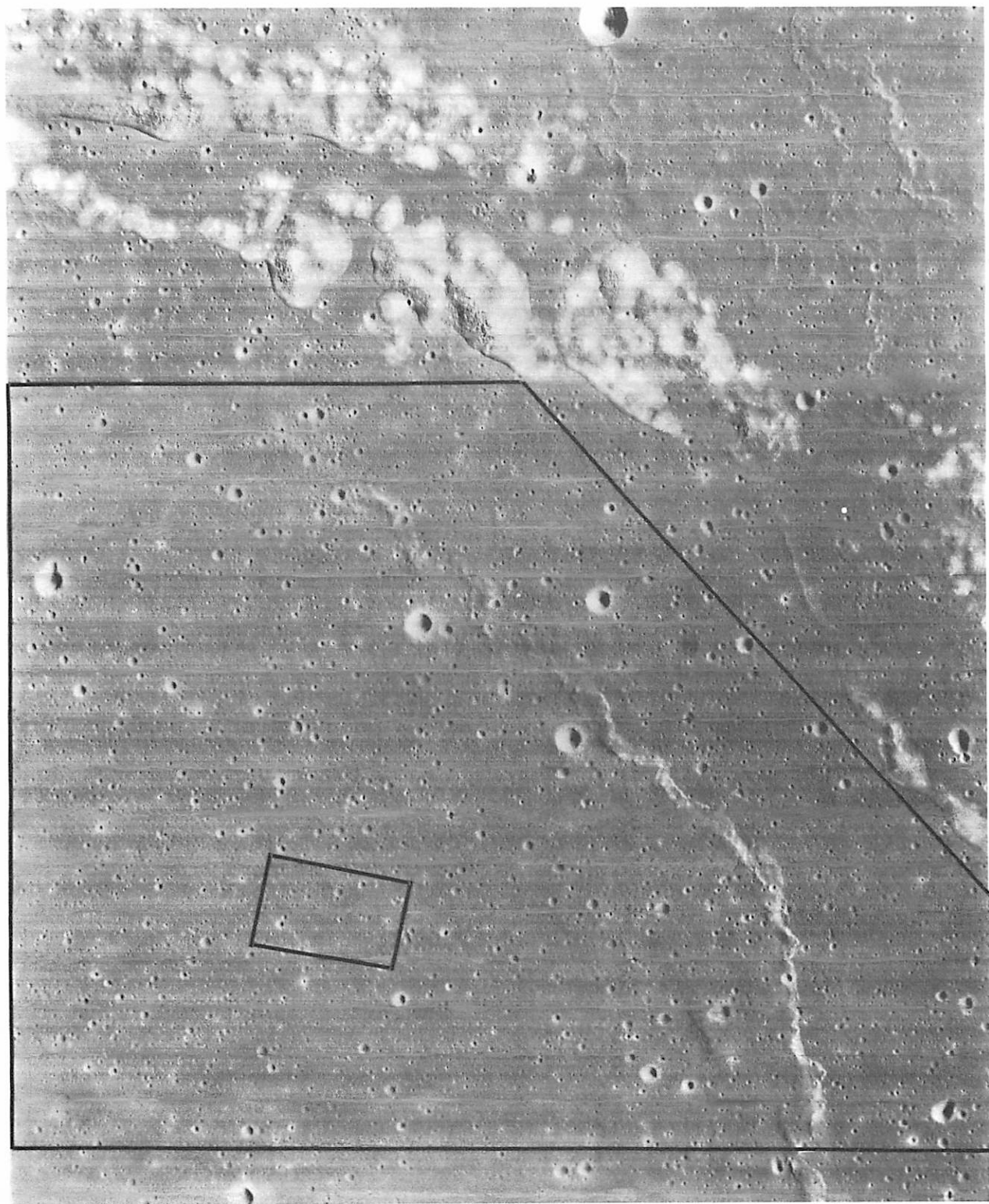


Fig. 2 Orbiter photograph I-M-194. The smaller marked area was used in extending the crater population curve, and is shown in greater detail in Fig. 3. (NASA photograph)

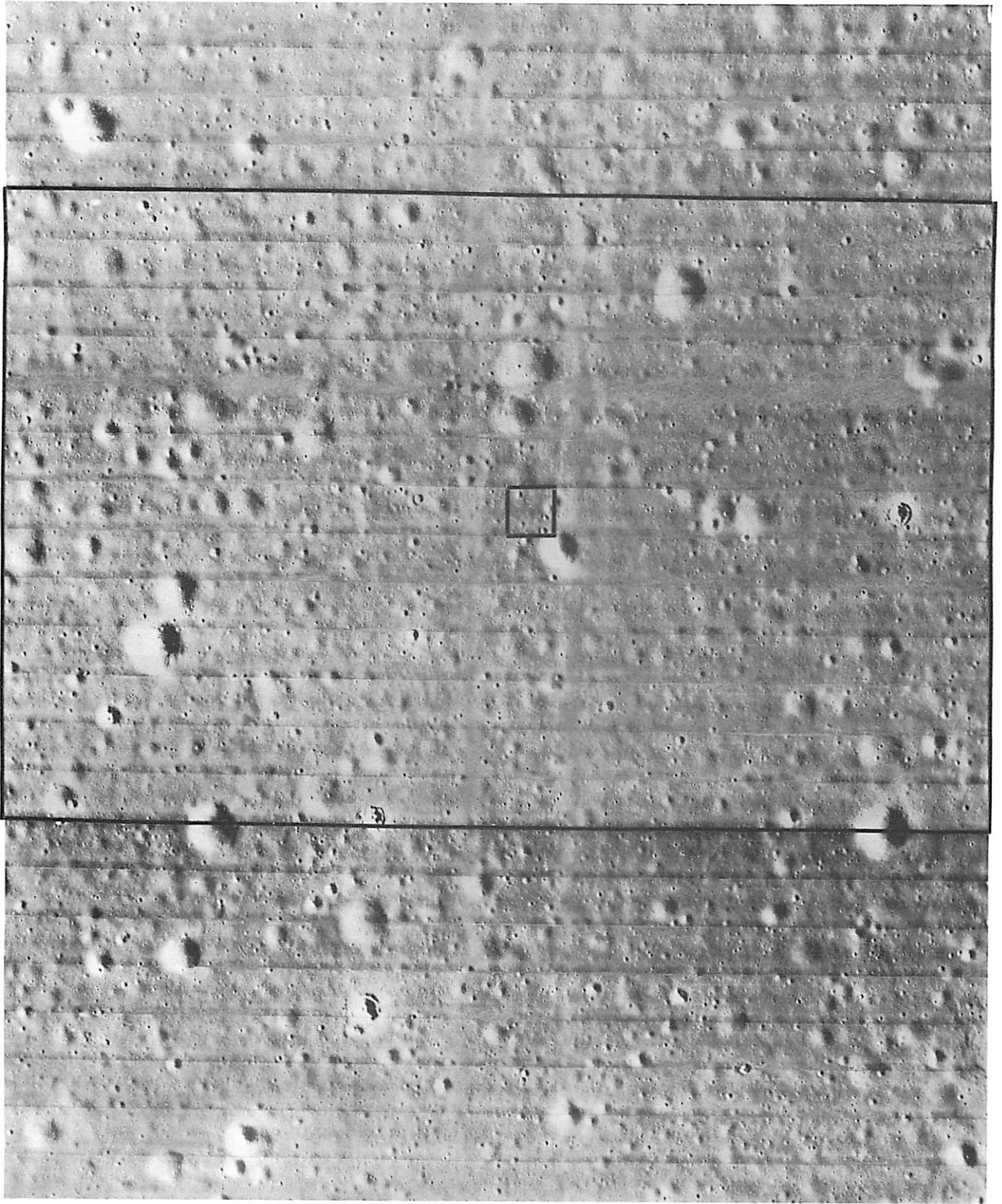


Fig. 3 Center portion of *Orbiter* photograph III-H-194. The larger marked area was used in the test for preferential chaining described in the text. The smaller marked area was used, greatly enlarged, in extending the crater population curve, and is shown in greater detail in *Fig. 4*. (NASA photograph)

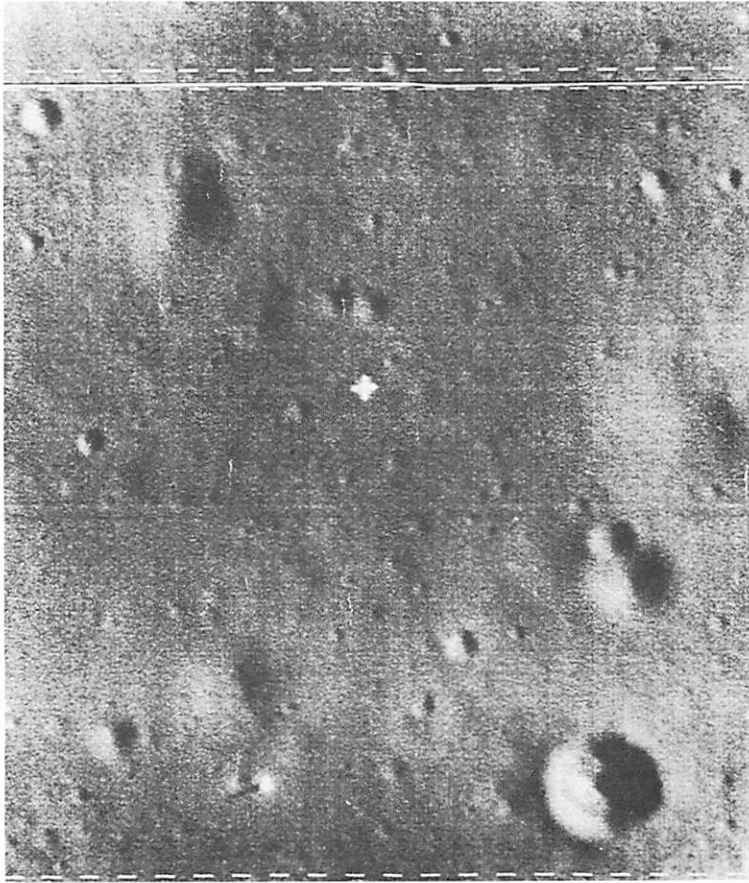


Fig. 4 Enlargement, from the original negative, of the smaller marked area in *Fig. 3*. (NASA photograph)

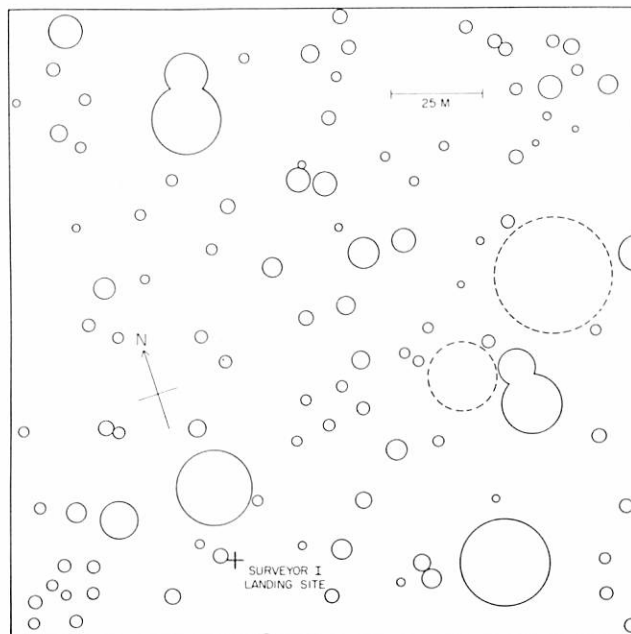


Fig. 5 Map of the area covered by *Fig. 4*. The horizontal scale is based upon shadow data.

is also observed on much sharper craters, which they attribute to impact.

This paper examines the crater distribution within and outside the ring as further evidence bearing on the chronology.

2. Extended Population Curves

Crater counts near the *Surveyor 1* landing site have been reported (Rennilson *et al* 1966; Fielder *et al* 1968). Rennilson *et al* utilized *Surveyor 1* records to analyze the diameter distribution in two small areas adjacent to the spacecraft. The first area was 6 m² about 4 m from the craft, and craters were counted between 1.6 and 25 cm. The second area was larger (47 m²) at a distance of about 7m, and was used in counting craters in the range 6.5 cm - 4 m. Of necessity, both areas were viewed very obliquely and were far from rectangular, resulting in a rapid change of scale with distance. For this reason, the smaller-diameter craters were undoubtedly under-represented in both counts. Allowing for this loss, Rennilson *et al*, concluded that the cumulative frequency distribution of craters in the range 1.6 cm - 4 m, at this locality, could be represented by

$$N = 720 \cdot d^{-1.80},$$

where N is the cumulative number of craters per m² and d is the crater diameter in cm.

Fielder *et al* investigated the region surrounding Flamsteed P as part of a more extensive project. The area designated by them as GA included the *Surveyor 1* landing site, a portion of the NE walls of Flamsteed P, and the gap in the northern walls of this ring (see Fig. 1). This area was defined by the boundaries of the ACIC map I-9.2 (100) and was counted twice by C. T., once from this map and once from a map by Fielder covering the entire extent of *Orbiter IV* photograph H-143. The resulting discrepancy in the counts (see Fig. 6) was tentatively attributed to the inclusion in Fielder's map of craters softer than those mapped by ACIC. The diameter range covered by these investigations was about 129 m-2 km.

In an attempt to span the gap, in the size range 4-130 m, three more counts were made on *Orbiter* photographs. The areas are indicated in Figs. 1-4 and the curves obtained are included with the four already described in Fig. 6. Care was taken not to include in these counts the walls of Flamsteed P. The two larger-scale areas were counted in the usual manner; the photographs used (I-M-194 and III-H-194)

were overlaid with clear acetate film, and crater centers marked with a felt-tipped pen as they were counted. The third area, Fig. 4, consisted of an enlargement (to 50 x 52 cm) of a section of one framelet of III-H-194, made from the original negative and containing *Surveyor 1*. The resolution of this area was therefore quite low, presenting an unusual problem. This area was overlaid with acetate and the estimated positions marked of the rims of all craters agreed upon by both investigators. The resulting map was used to make the final count. This map is given in Fig. 5 for comparison with Fig. 4. The scale of this count was assigned by shadow measurements of the spacecraft.

Horizontal scales are thus based on three distinct sets of estimates. Rennilson *et al* assigned their scale by an unspecified method. Because of difficulties with perspective, the resulting measurements must be regarded as approximate. Shadow data were utilized for the single area as described above. The remaining counts were consistent with one another and were based on the direct measurement of standard sizes of features in the larger scale photograph. There is some degree of inconsistency between the various measures. For instance, the scale of *Orbiter* photograph III-H-194 was calculated to be 9.2 m/mm from shadow data but 12.9 m/mm by comparison with large-scale photographs. To achieve maximum internal consistency with the other curves, the latter value was used.

It will be noted that the new count for large diameters agrees closely with the data obtained by Fielder *et al* from the ACIC map.

Examination of Fig. 6 reveals an anomaly for craters with diameters 2-4 m, possibly due to small diameter losses from the poor resolution of the print used. Further, if the curve obtained from Fielder's map of area GA is disregarded, the data may be represented by two straight line segments:

$$N = 4.84 \times 10^5 D^{-2.12} \quad 1.7 \text{ cm} < D < 80 \text{ m}$$

$$\text{and } N = 3.80 \times 10^6 D^{-3.10} \quad 80 \text{ m} < D < 2 \text{ km}$$

where N is the cumulative number of craters/1000 km² greater than diameter D meters. The lines corresponding to these equations are included in both Figs. 6 and 7.

3. Position Distribution of Craters

The positional distribution of points in a plane (or of crater centers on a plane area of the Moon) may be examined in two complementary ways.

Searches may be made either for large changes in number density with relation to position; or for specific patterns, usually chains, which do not appreciably disturb the overall number density.

Fielder *et al.* (1968) applied both methods to mare surfaces on the near-side of the moon, and as part of this project investigated the area covered by Fig. 1, with the following results:

- 1) The crater density within Flamsteed P in the range 129 m-3.7 km is appreciably lower than on the mare surface outside the ring (see Fig. 7).
- 2) The change in crater density occurs at the boundary of the ring and is quite sharp, except at the northern edge where the transition is less abrupt and the boundary ill-defined.
- 3) While there are regional crater alignments in the area of Fig. 1 as a whole, no alignments are found in the interior of Flamsteed P.
- 4) Between 48% and 80% of craters within the whole region were estimated as being of internal origin.

Fielder *et al.* examined area GA (cf. Fig. 1) which includes much of the NE wall and a small amount of external mare surface, but is not truly representative of the interior. For this reason, counts were made on a map of crater positions *inside* Flamsteed P showing craters of diameters 12.9 m-280 m (cf. Fig. 3). The resulting diagram of Index of Dispersion, V , versus Azimuth θ , is shown in Fig. 8. This method is discussed in Fielder and Marcus (1967), Fryer (1968), and Fielder *et al.* (1968), and only a brief review will suffice here for the interpretation of Fig. 8.

For a random set of points, the curve of V versus θ lies closely along the line $V = 1$. Any form of non-randomness will cause the curve to deviate from this line, usually by an increase in V . The test enables peaks in the curves obtained to be interpreted as evidence of *chaining* parallel to the indicated azimuths, a general increase of level of the curve as evidence for *clustering* of crater centers with no preferred azimuth; and a general *lowering* of the curve as evidence that the crater centers are more uniformly arranged than expected in a random distribution.

The curve obtained for the new test area lies mostly below $V = 1$, indicating a tendency toward a distribution more uniform than expected from impacts.

4. Comparison with Ranger Crater Counts

It is interesting to compare the crater distributions obtained with those derived in the same diameter range for other regions. The *Ranger* results are of special interest.

Trask (1966) gives counts from *Rangers VII-IX*. Of his curves, that for *Ranger VII* (cf. Fig. 7) resembles most closely that obtained for *Surveyor I*. Both are well represented by two straight-line segments. *Ranger VII* shows lower crater densities than *VIII* and *IX*, possibly due to its higher angle of illumination. Trask combines data for very small craters obtained from *Ranger* records with data on larger craters from densely-covered uplands, to derive the empirical geometric saturation diameter-distribution:

$$N = 10^{10.9} d^{-2}$$

where N is the cumulative number of craters per 10^6 km² larger than diameter d meters. This line is also plotted in Fig. 7 and marked "steady-state." Craters a few cm in diameter appear in equilibrium at the *Surveyor I* landing site. Departures from the saturation distribution increase with increasing diameter.

Le Poole (1966), in a study of crater distributions of *Rangers VII-IX*, found that the curves for the three areas were identical for $d > 7$ m [on this basis Kuiper (1966) concluded that the three *Ranger* areas were composed of similar mare terrain except for the uppermost 1-2 meters that had been fragmented since the mare formation]. Le Poole divided the composite curve into three sections with breaks occurring at 22 m and 120 m.

Chapman (1968) also investigated the *Ranger* records, attempting to distinguish between the various morphological crater type first recognized in the *Ranger* program (JPL Tech. Report 32-700, 1965; 32-800, 1966). He confirmed the earlier *Ranger* results, that the crater types range from sharp impacts to collapse or "sink-hole" features.

Cross (1966) combined his own counts on *Ranger* records with measurements made on three areas of Wilkins (1946) map of the Moon. His crater densities are lower than those by Trask, possibly due to lower print quality. Cross concludes that an inverse-square law adequately describes the counts for all three missions for the diameters covered. His curves for *Ranger VIII* and *IX* are included in Fig. 7.

Hartmann (1968) investigated a variety of areas and finds variations in crater density from one mare to another by a factor of up to 2.5, with the "knee"

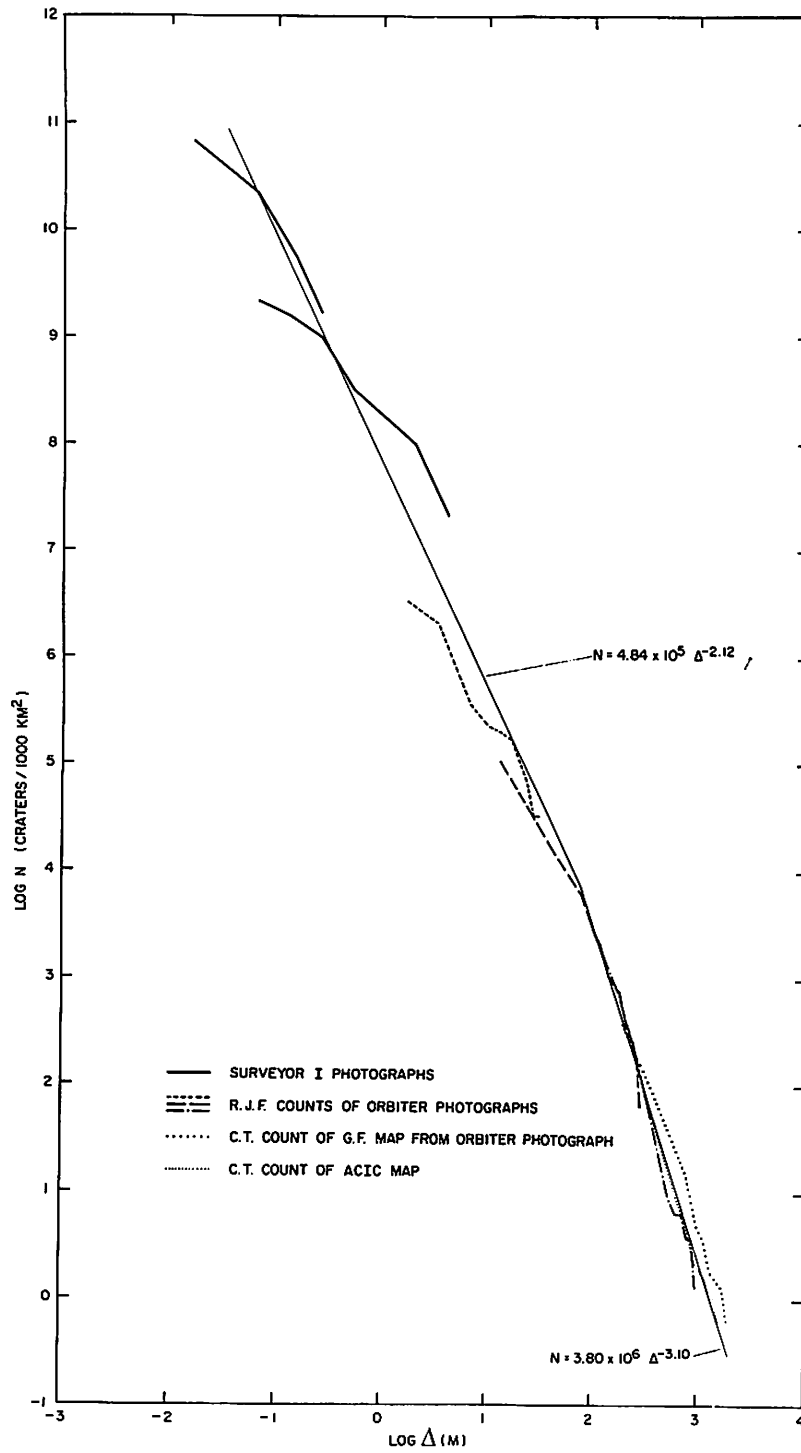


Fig. 6 Total population curve of *Surveyor I* landing site, cumulative frequency N versus diameter Δ meters.

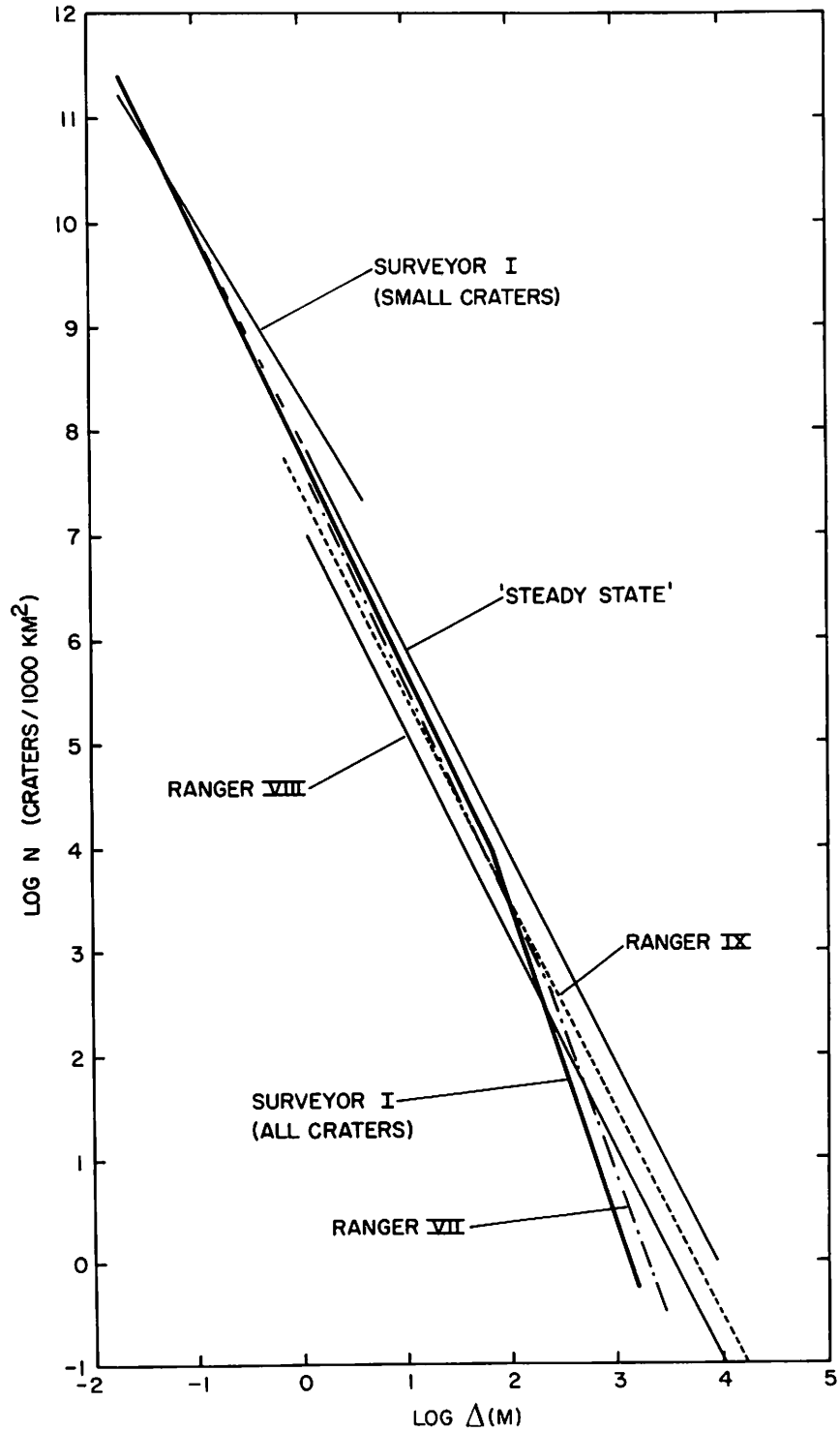


Fig. 7 Surveyor I population curve compared with a sample of equivalent data by other workers (see text). Cumulative frequency, N , versus diameter Δ meters.

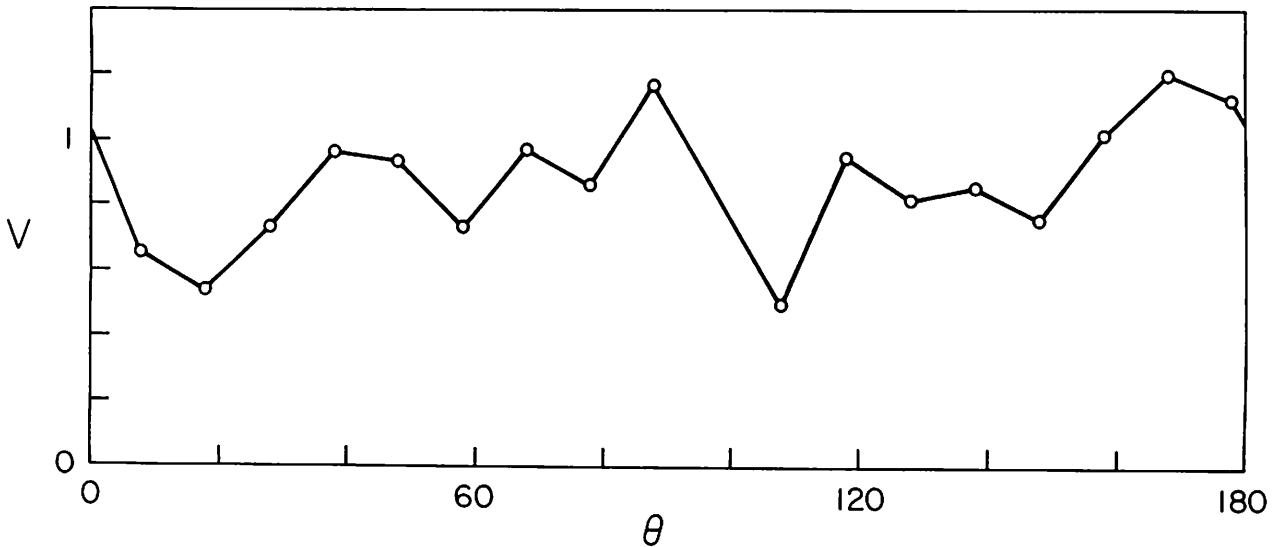


Fig. 8 Index of Dispersion, V , versus Azimuth, θ , of the area indicated in Fig. 3 (see text).

occurring typically at several hundred meters diameter. He concludes that in most areas only craters larger than about 2 km diameter define the "primary" crater distribution.

The lack of crater chains within the boundaries of Flamsteed P is unusual. Fielder (1968) detected on the *Ranger VIII* and *IX* records evidence for chaining. The absence of detectable chains within Flamsteed P indicates a somewhat different history as compared to the *Ranger VIII* and *IX* impact sites.

5. Interpretations and Conclusions

The evidence quoted leads to the conclusion that the interior of Flamsteed P is "young" compared to both other mare regions (*Ranger VII*, *VIII*) and its immediate surroundings. Since Fig. 8 gives no indication of crater chaining, it would permit the assumption that all craters considered are of impact origin. This then would indicate an age of about half that derived by Fielder *et al.* for the area immediately external to Flamsteed P on the N.E. side. On the other hand, the mean level of the (V, θ) curve in Fig. 8 is below $V = 1$. We interpret this fact as indicating the presence of numerous collapse depressions distributed quasi-uniformly over the surface. The number of true impacts, both primary and secondary, is therefore very low and the derived relative age still less.

Marshall (1963) following the usual assumption for "ghost" craters, regarded Flamsteed as being youngest; the mare surface inside and out, as being older and contemporaneous; and the walls of Flam-

steed P as oldest. We agree that Flamsteed (overlapping Flamsteed P) is the youngest structure, but have found that the interior plain is younger than the exterior mare. Now, on the hypotheses of O'Keefe *et al.* (1967) and Fielder (1967), the walls would be the younger than the interior plain. On the other hand, the younger age of the interior plain could well be due to its origin from the ring itself.

Acknowledgments. This work is part of the LPL interpretive program supported by JPL/NASA Contract No. 952166.

REFERENCES

- Chapman, C. R. 1968, "Interpretation of the Diameter-Frequency Relation for Lunar Craters Photographed by *Rangers VII*, *VIII*, and *IX*," *Icarus*, 8, pp. 1-22.
- Cross, C. A. 1966, "The Size Distribution of Lunar Craters," *M.N.R.A.S.*, 134, pp. 245-252.
- Fielder, G. 1967, "Volcanic Rings on the Moon," *Nature*, 213, pp. 333-336.
- Fielder, G., and Marcus A. 1967, "Further Tests for Randomness of Lunar Craters," *M.N.R.A.S.*, 136, pp. 1-10.
- Fielder, G. 1968, "Linear Arrays of Craters on the *Ranger* Photographs," *Planet. Space Sci.*, 16, pp. 501-508.
- Fielder, G., Fryer, R. J., Titulaer, C., "Origin of the Smaller Craters in the Lunar Maria Based on *Orbiter* Photography," *Comm. LPL* (in press).

- Fryer, R. J. 1968, "Crater Alignments in the Flamsteed Region of the Moon," *Planet. Space Sci.*, **16**, pp. 809-814.
- Guest, J. E., and Fielder, G. 1968, "Lunar Ring Structures and the Nature of the Maria," *Planet. Space Sci.*, **16**, pp. 665-673.
- Hartmann, W. K. 1967, "Extrusive Lunar Ring Structures?" *Science*, **157**, p. 841.
- Hartmann, W. K. 1968, "Lunar Crater Counts," *Comm. LPL*, **7**, Nos. 116-119, pp. 125-156.
- Kuiper, G. P. 1966, "Interpretation of the *Ranger* Records," (JPL T. R. No. 32-800), pp. 35-248 (also, *Comm. LPL*, **4**, pp. 1-70)
- Le Poole, R. S. 1966, "Frequency of Post-Mare Craters," in *Ranger VIII and IX, Part II. Experimenters' Analyses and Interpretations*, (JPL T. R. No. 32-800), pp. 161-172.
- Marshall, C. H. 1963, "Geological Map and Sections of the Letronne Region of the Moon," [U.S. Geological Survey, Misc. Geol. Inv. Map (LAC-75)].
- O'Keefe, J. A., Lowman, P.D., and Cameron, W. S. 1967, "Lunar Ring Dykes from Lunar *Orbiter* 1," *Science*, **155**, pp. 77-79.
- Rennilson, J. J., Dragg, J. L., Morris, E. C., Shoemaker, E. M., and Turkevich, A. 1966, "Lunar Surface Topography," in *Surveyor I Mission Report. Part II, Scientific Data Results*, (JPL T. R. No. 32-1023), pp. 7-44.
- Trask, N. J. 1966, "Size and Spatial Distribution of Craters Estimated from the *Ranger* Photographs," in *Ranger VIII and IX, and Part II. Experimenters' Analyses and Interpretations*, (JPL T. R. No. 32-800), pp. 252-262.
- Whitaker, E. 1968, Private Communication.